

Magnetolectric 'spin' on stimulating the brain

Aim: The *in vivo* study on imprinting control region mice aims to show that magnetolectric nanoparticles may directly couple the intrinsic neural activity-induced electric fields with external magnetic fields. **Methods:** Approximately 10 μg of $\text{CoFe}_2\text{O}_4\text{-BaTiO}_3$ 30-nm nanoparticles have been intravenously administered through a tail vein and forced to cross the blood-brain barrier via a d.c. field gradient of 3000 Oe/cm. A surgically attached two-channel electroencephalography headmount has directly measured the modulation of intrinsic electric waveforms by an external a.c. 100-Oe magnetic field in a frequency range of 0–20 Hz. **Results:** The modulated signal has reached the strength comparable to that due the regular neural activity. **Conclusion:** The study opens a pathway to use multifunctional nanoparticles to control intrinsic fields deep in the brain.

Keywords: magnetolectric nanoparticles • nanoengineering the brain • noninvasive brain stimulation

A neural network can be considered as a complex bioelectric circuit made of many neurons connected through chemical and electrical synapses formed between axons and dendrites [1–3]. The signaling in the network is electric-field driven and based on a highly collective system of electric charges, neurotransmitters and action potentials. The ability to remotely incite specific neuronal excitations deep in the brain with the purpose to artificially stimulate selective regions of the network remains an important open question in neural engineering [4]. Furthermore, the ability to control the central nervous system (CNS) at micro- or even nanoscale could provide unprecedented control of specific functions and enable highly personalized 'pin-point' treatment of neurodegenerative diseases such as Parkinson's disease, essential tremor, epilepsy and others [5,6].

The current brain stimulation technology is operated at macroscale and often relies on highly-invasive direct-contact-electrode techniques such as deep-brain stimulation (DBS) [7–9]; it can be noted that DBS is one

of only a few neurosurgical methods allowed for blinded studies. There are also noninvasive brain stimulation methods; these include repetitive transcranial magnetic stimulation (rTMS) [10,11] and transcranial direct current stimulation [12,13]. Though rTMS and transcranial direct current stimulation indeed represent major technological advances in noninvasive brain stimulation, the depth and locality of focusing are strongly limited in both methods [14–16]. In rTMS, relatively high intensity magnetic fields (on the order of 10,000 Oe) are required to stimulate regions deep in the brain; however, high intensity magnetic fields, especially in the a.c. mode, may lead to excessive energy dissipation or other destructive side effects [17]. The required high external magnetic field can be explained by the relatively weak coupling between the magnetic field and the local electric currents in the neural system.

With the above said, one can identify the following engineering bottleneck. On one hand, using electric fields one can achieve adequate brain stimulation; however, the

Rakesh Guduru^{1,2}, Ping Liang³, J Hong⁴, Alexandra Rodzinski¹, Ali Hadjikhani², Jeffrey Horstmyer⁵, Ernest Levister⁶ & Sakhrat Khizroev^{*1,2,5}

¹Department of Cellular Biology & Pharmacology, Herbert Wertheim College of Medicine, Florida International University, Miami, FL 33199, USA

²Department of Electrical & Computer Engineering, Florida International University, Miami, FL 33174, USA

³Department of Electrical & Computer Engineering, University of California, Riverside, CA 92521, USA

⁴Department of Electrical Engineering & Computer Science, University of California, Berkeley, CA 94720, USA

⁵Neuroscience Centers of Florida Foundation, Miami, FL 33124, USA

⁶School of Medicine, University of California, Irvine, CA 92697, USA

*Author for correspondence:

Tel.: +1 305 348 3724

khizroev@fiu.edu

need to establish direct contact with individual neurons makes the electric field stimulation highly invasive. It is hard to see how such a physical direct contact with each of the 75 billion neurons in the brain can be achieved. On the other hand, magnetic fields can penetrate through the brain without being significantly distorted by the local microenvironment and therefore can be used for externally controlled stimulation; however, inadequately weak coupling between external magnetic fields and intrinsic neural activity-induced electric currents makes such stimulation relatively inefficient and consequently inadequate for being used for local stimulation deep in the brain.

One potential solution for enabling high-efficacy remote control of the neural activity deep in the brain would be to use conventional magnetic nanoparticles (MNs) to locally amplify the magnetic field and thus enhance the effective coupling to local electric currents [18]. An even more dramatic solution could be achieved by using a novel class of functional nanoparticles known as magnetoelectric nanoparticles (MENs) [19–21]. Under an equivalent magnetic field exposure, MENs not only can amplify the local magnetic field but also generate an additional local electric field. The field is generated due to the nonzero magnetoelectric (ME) effect, which originates from an intrinsic coupling between electric and magnetic fields in MENs. As a result, when administered in the brain, MENs can serve as nanoscale sites which, when exposed to a relatively low external magnetic field (in the range of 100–1000 Oe), generate local electric fields (on the order of 1000 V/m or higher) to provide direct external access to the internal (bioelectric) neural circuits. In other words, MENs enable a unique way to combine the advantages of both the high efficacy of the electric fields and the external-control capability of the magnetic fields and therefore open a novel pathway to control the brain.

To the best of our knowledge, this paper for the first time presents results of an animal study to demonstrate the use of toxicity-free MENs to stimulate the brain via application of low external magnetic fields.

Methods

Fabrication of toxicity-free MENs

Details on the fabrication of toxicity-free MENs were described in our recently published comprehensive studies [22,23]. The basic structure of CoFe_2O_4 - BaTiO_3 core-shell 30-nm MENs was synthesized according to the following steps: 0.058 g of $\text{Co}(\text{NO}_3)_2 \cdot 6\text{H}_2\text{O}$ and 0.16 g of $\text{Fe}(\text{NO}_3)_3 \cdot 9\text{H}_2\text{O}$ were dissolved in 15 ml of deionized water; 5 ml of aqueous solution containing 0.9 g of sodium borohydride and 0.2 g of polyvinylpyrrolidone was added at 120°C for 12 h to obtain

CoFe_2O_4 nanoparticles; BaTiO_3 precursor solution was prepared by adding 30 ml of deionized water containing 0.029 g of BaCO_3 and 0.1 g of citric acid to 30 ml ethanolic solution containing 1 g of citric acid and 0.048 ml of titanium (intravenous[ly] [iv.]) isopropoxide; as-prepared CoFe_2O_4 nanoparticles (0.1 g) were added to the 60 ml of BaTiO_3 precursor solution and sonicated for 120 min; the resulted dispersed nanoparticles were dried on hot plate at 60°C for 12 h, while stirring at 200 rpm; the obtained powder was heated at 780°C for 5 h in a box-furnace and cooled at 52°C min^{-1} to obtain 30 nm-sized CoFe_2O_4 - BaTiO_3 core-shell MENs. To eliminate toxicity at least in *in vitro* studies, the nanoparticles were surface functionalized by a 2-nm thick coating of glycerol mono-oleate (GMO) according to the following steps: GMO-MENs were prepared by incubating 0.1 mg of GMO with 5 mg of MENs in 5 ml of PBS (pH 7.4) buffer for 12 h to achieve uniform surface modification, the solution was slowly agitated during incubation; the solution was centrifuged at 20,000 rpm for 20 min at 10°C to remove excess GMO; the obtained pellet was resuspended in ethyl acetate:acetone (70:30) solution and recentrifuged three-times to obtain GMO-MENs; surface-modified MENs were lyophilized and stored at 4°C until further use. The particle size distribution was measured by a Zetasizer Nano series that uses the standard dynamic light scattering approach. The measured zeta potentials for nonfunctionalized and functionalized (with GMO) MENs were -45 ± 1.72 mV and -41.6 ± 0.26 mV, respectively.

An *in vitro* cytotoxicity of MENs

An *in vitro* cytotoxicity study was performed using XTT assay (sodium 2,3-bis(2-methoxy-4-nitro-5-sulfophenyl)-5-[(phenylamino)-carbonyl]-2H-tetrazolium inner salt) according to the manufacturer's protocol (ATCC), as previously discussed [22,23]. The assay was performed on human astrocyte cells and peripheral blood mononuclear cells for neuronal and peripheral cytotoxicity, respectively. The results of the XTT assay (performed in triplicates, $n = 3$) indicated no significant toxicity on both cell types, human astrocyte and peripheral blood mononuclear cells, respectively, in the GMO-MEN concentration range from 0 to 200 $\mu\text{g}/\text{ml}$, as summarized in the chart in **Supplementary Figure 1** (please see online at <http://www.futuremedicine.com>).

Animal studies: electroencephalography setup

To directly track the electric field response in the brain under different experimental conditions of this study, a two-channel electroencephalography (EEG) head-mount was surgically implanted into the head of an

imprinting control region (ICR) mouse (~2-month old females) (Supplementary Figure 2A). As described below in more detail, four solid electrodes, two for each channel, were surgically attached to the skull via four nonmagnetic stainless steel screws to physically touch the brain in four different points over the cerebral cortex. This setup allowed to directly measure local electric signals in the brain's neural network in response to external-magnetic-field-activated nanoparticles. During the measurements, mice were kept under general anesthesia using inhalatory isoflurane (~1.5%) through a stereotaxic nosecone, as shown in Supplementary Figure 2B. The nanoparticles were introduced into the bloodstream via iv. injection through the tail vein. The concentration of the nanoparticle saline solution was approximately 200 µg/ml. The amount of the solution injected into the tail vein was approximately 0.05 ml (~10 µg of nanoparticles). After the injection, to transfer the nanoparticles from the bloodstream into the brain across blood–brain barrier (BBB), a magnetic field gradient of approximately 3000 Oe/cm was applied for approximately 30 min using a permanent neodymium magnet placed over the top part of the head for approximately 30 min, as shown in a photograph in Supplementary Figure 2B. It can be noted that because the main focus of this study was to understand the novel properties of MENs in the neural microenvironment in the brain, no significant emphasis was made on transferring all the iv.-administered nanoparticles across BBB. Generally, it is believed that approximately 10% of iv.-administered nanoparticles transfer into the brain [24]. It should be noted that in this particular case, this estimate might be conservative considering a 'magnetic-field-gradient pull' was used to force the nanoparticles to cross BBB.

After the 'smart' nanoparticles were delivered in the brain, the response of the two-channel EEG headmount to local neural electric signals due to the nanoparticles' magnetic (with MNs) or magnetoelectric (with MENs) response was studied via application of a low-energy a.c. magnetic field with a magnitude of 100 Oe and a frequency in a range from 0 to 20 Hz. The a.c. field was generated by a 1-inch electromagnetic multiturn coil that was placed approximately 0.5 cm away from the head. The field profile generated by the standard coil setup can be easily calculated and therefore was well predictable and controlled. To avoid any potential interference of the fields due to residual nanoparticles, for each nanoparticle type and dosage, a separate mouse was used.

Animal studies: surgery

The current *in vivo* studies were performed in accordance with the guidelines of Institutional Animal Care

and Use Committee (IACUC) # FIU: 13–045. The ICR mice under study were purchased at Jackson Laboratory for Genomic Medicine. Mice were sedated in a 5% Isoflurane environment in an induction chamber before they were placed on a stereotaxic apparatus for further procedures under general anesthesia with a 2% Isoflurane flow through a gas mask. A surgical incision was made on the head to expose the periosteum. A two-channel EEG headmount was affixed onto the periosteum using a surgical glue (cyanoacrylate) and four 3-mm stainless steel screws which also served as EEG electrodes. The two channels were separated by approximately 5 mm. The headmount was placed approximately 3 mm anterior to bregma, so that all the four screws would rest on the cerebral cortex region of the mouse brain. After the electric contact between the headmount and the EEG electrodes was re-enhanced via application of silver epoxy, the implant was further secured via a dental acrylic. As a postoperative care, every 8 h for three days, mice were administered with analgesics (Buprenex, 0.15 mg/kg) through subcutaneous injection and antibiotics (Baytril 2.27 mg/ml) through drinking water. Mice were given two weeks for recovery before conducting further experiments. After completion of the study, the mice were sacrificed by CO₂ hypoxia followed by cervical dislocation according to the AVMA guidelines.

Cryo-sectioning of brain tissue

Whole brains were dissected and immersion-fixed in 4% paraformaldehyde (wt/vol; dissolved in PBS solution) at 4°C overnight with gentle shaking. Then, the brains were washed three-times in PBS solution, cryoprotected with PBS-buffered 30% sucrose and embedded in O.C.T. medium (Tissue-Tek). Serial 10-µm-thick sections along the sagittal plane of the right and left cerebral hemispheres were cut using a Leica CM3050 Cryostat. Atomic force microscopy (AFM) imaging was performed directly on the cryosectioned samples.

Scanning electron microscopy sample preparation

Cryosectioned mouse brain tissue samples were fixed by a 3% glutaraldehyde buffer solution (0.1 M PBS) at room temperature for 2 h. After the samples were washed three-times with a 0.1 M PBS (pH 7.2), they were immersed in a 1% osmium tetroxide solution (250 mg of OsO₄ in 25 ml of 0.1 M PBS, pH 7.2) for 2 h at room temperature in dark environment followed by, washing three-times with a 0.1 M PBS, with a pH of 7.2. After washing, dehydration was induced by graded ethanol solution in water for 5 min for the following concentration sequence: 30, 50, 70, 80, 90, 95 and 100%. Then, the samples were dried in a graded

HMDS ethanol solution of 30 and 50% for 20 min and 100% for approximately 14 h. Thus prepared samples were mounted on a SEM specimen stub with a carbon tape for imaging.

Vibrating sample magnetometry

A room-temperature Lakeshore vibrating sample magnetometer (VSM) with a 3-T magnetic field sweep was used to measure key magnetic properties of nanoparticles under study including the magnetization saturation and the magnetic coercivity.

Scanning probe microscopy

Scanning probe microscope Multimode was used to measure AFM and magnetic force microscopy (MFM) images of nanoparticles under study. The MFM images were obtained with a CoCr-based hard magnetic nanoprobe at a scan height of 10 nm.

Transmission electron microscopy

Phillips CM-200 200 kV TEM with Energy Dispersive Spectroscopy (EDS) option was used to obtain TEM images and EDS profiles.

Results

A typical TEM image of the synthesized 30-nm MENs, with a clearly visible core-shell structure, is shown in [Figure 1A](#). The core and shell were made of the magnetic-moment enhancing CoFe_2O_4 ferromagnetic spinel and magnetoelectricity inducing BaTiO_3 perovskite nanostructures, respectively. The composition was confirmed through energy-dispersive spectroscopy. These nanostructures have a ME coefficient that can be varied from 1 to 100 $\text{mV cm}^{-1} \text{Oe}^{-1}$ through substitution of transition metals by other elements from the same series. A typical room-temperature magnetic hysteresis loop, which was measured via VSM, is shown in [Figure 1B](#). The curve indicates a ferromagnetic nature of the magnetic component. The saturation magnetization and the magnetic coercivity of these nanoparticles were on the order of 1 emu/g and 100 Oe, respectively. [Figure 1C](#) shows a MFM image of MENs subjected to an external electric field of approximately 100 V/cm along X-direction. The image, obtained with a low-moment probe, shows an electric-field induced dipole moment in the same orientation.

Typical scanning electron microscopy (SEM) images of brain sections in a sagittal plane for two mice, including a sample with MENs and a sample without any MENs (control), respectively, are shown in [Figure 2A](#) [22,23,25]. A pair of atomic and magnetic force microscopy (AFM and MFM) images of a 'zoomed-in' region of the brain section with MENs is shown in [Figure 2B](#).

The EEG waveforms and their respective frequency spectra (Fourier transforms) for the response to a 100-Oe external magnetic field at frequencies of 0, 5, 10, 15 and 20 Hz are shown in [Figure 3](#). The frequency range was limited by the available electronics. The resulting modulation by the a.c. magnetic field can be clearly observed. The modulated periodic signal on the order of 1 mV is comparable to the magnitude of the unperturbed original signal in the brain. As seen in the frequency response, indeed the new modulated electric-field component is at the same frequency as the external a.c. magnetic field applied by the coil setup, as described above. The two channels show comparable signals.

Thus determined intrinsic electric field modulation amplitude was measured as a function of the external a.c. magnetic field amplitude, as shown in [Figure 4](#). The dependence saturated at approximately 100 Oe field, which was on the order of the coercivity field of the MEN system under study.

To confirm that the modulated effect indeed resulted from the presence of MENs, the following control measurements were performed.

In the first control measurement, EEG waveforms were recorded without introducing any nanoparticles in the brain. The typical EEG waveforms at five values of the a.c. frequency, 0, 5, 10, 15 and 20 Hz, respectively, are shown in [Supplementary Figure 3](#) (left). The frequency spectrum (Fourier Transform) of the signal for each a.c. frequency response is shown in [Supplementary Figure 3](#) (right). It is worth noting that the waveforms were not visibly affected by application of the a.c. magnetic field in the frequency (<30 Hz) and amplitude ranges (<300 Oe) under study.

In the second control measurement, MENs were substituted with the same amount of conventional MNs. As conventional MNs, 30-nm CoFe_2O_4 nanoparticles were injected in the brain at the equivalent dose of 10 μg . The saturation magnetization of these nanoparticles was on the order of 100 emu/g (via VSM measurements), compared with approximately 1 emu/g for MENs. The typical EEG waveforms from the two EEG channels and their frequency spectra for the response to a 100-Oe external magnetic field at frequencies of 0, 5, 10, 15 and 20 Hz are shown in [Supplementary Figure 4](#) (left) and (right), respectively. It could be noted that like the first control measurement (without any nanoparticles in the brain), the waveforms were barely affected by the application of an a.c. magnetic field. Here, one should mention that the experiment could not completely exclude the effects due to MNs; it just shows that the sensitivity of the current setup ($\sim 50 \mu\text{V}$) was not sufficient for detecting the MN-induced signal under the current experimental conditions.

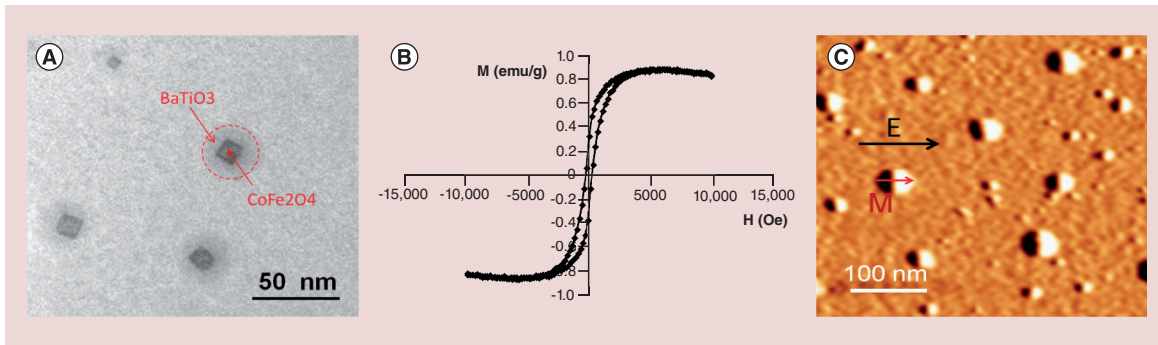


Figure 1. Nanoparticle characterization. (A) Transmission electron microscopy image of magnetoelectric nanoparticles (MENs). The core-shell structure can be seen. (B) M-H loop of MENs measured via vibrating sample magnetometry at room temperature. (C) Magnetic force microscopy image of MENs exposed to an external electric field E_x of 100 V/cm. M stands for the magnetization. For color figures, please see online at www.futuremedicine.com/doi/full/10.2217/NNM.15.52

Discussion

The main goal of this study was to demonstrate through *in vivo* studies on ICR mice that MENs, when administered in the brain, could enable externally controlled noninvasive deep-brain stimulation [25]. In the main experimental setup, iv.-injected nanoparticles were forced via application of a magnetic field gradient of approximately 3000 Oe/cm to enter the brain by crossing BBB (Figure 3). Like conventional MNs, MENs have a nonzero magnetic moment and therefore could be controllably transferred across the BBB via application of a remote magnetic field gradient force, as was confirmed through two types of imaging, SEM and AFM/MFM, respectively, to observe the presence of MENs in brain sections (Figure 2). The MENs' coercivity on the order of 100 Oe (Figure 1B) was smaller than the stray field generated by a typical CoCr-based MFM probe and therefore during imaging the nanoparticles were always magnetized in the same orientation as the nanoprobe's magnetic moment. The dark color for the nanoparticles in the MFM image reflects the attractive force between the nanoparticles and MFM nanoprobe, which is in agreement with their relative orientations.

It could be noted that the particle distribution was relatively inhomogeneous, as we would expect. From the signal-to-noise perspective, to have a substantial portion of the brain to be sensitive to the stimulating effect, it would be preferred to have as many nanoparticles per neuron as possible without destructing the operation of the brain. A dose of 10 μg of MENs (equivalent to ~ 20 billion nanoparticles, assuming the atomic density of a 30-nm nanoparticle to be on the order of 5 g/cc) was administered in the blood stream through an iv. injection in a mouse tail vein. Considering 75 million neurons per brain, on average there were hundreds of particles per neurons. It should be noted that the current estimate is very approximate. In the future, a more comprehensive *in vivo* study must

be conducted to understand the detailed metabolism of the nanoparticles. A special EDS-based analysis of the nanoparticle distribution in different organs has been developed to study the biodistribution of MENs of different compositions, sizes and shapes in different organs in different time intervals after the injections. This study will be discussed in a separate paper in the near future. An example of the biodistribution analysis of nanoparticles in a kidney tissue is shown in Supplementary Figure 5. Today, iron oxide magnetic nanoparticles are used as image contrast enhancement agents in magnetic resonance imaging [26,27]. It could

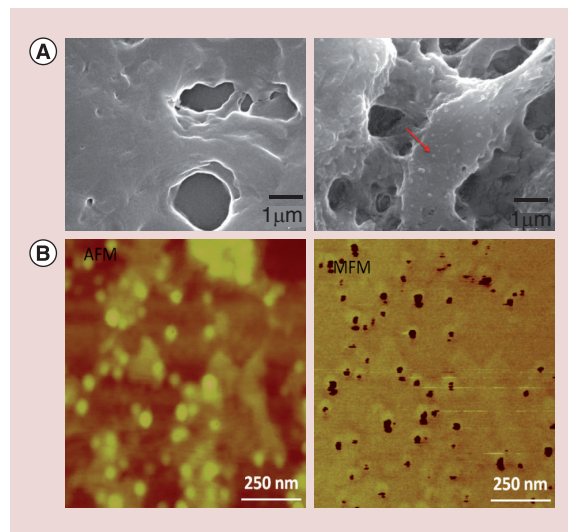


Figure 2. Detection of magnetoelectric nanoparticles deep in the brain. (A) Scanning electron microscopy images of sagittal brain sections of two mice: (left) without magnetoelectric nanoparticles (MENs) in the brain and (right) with MENs in the brain. The red arrow points to a MEN. (B) Atomic force microscopy (left) and magnetic force microscopy images of a small region containing a relatively dense concentration of MENs. AFM: Atomic force microscopy; MFM: Magnetic force microscopy.

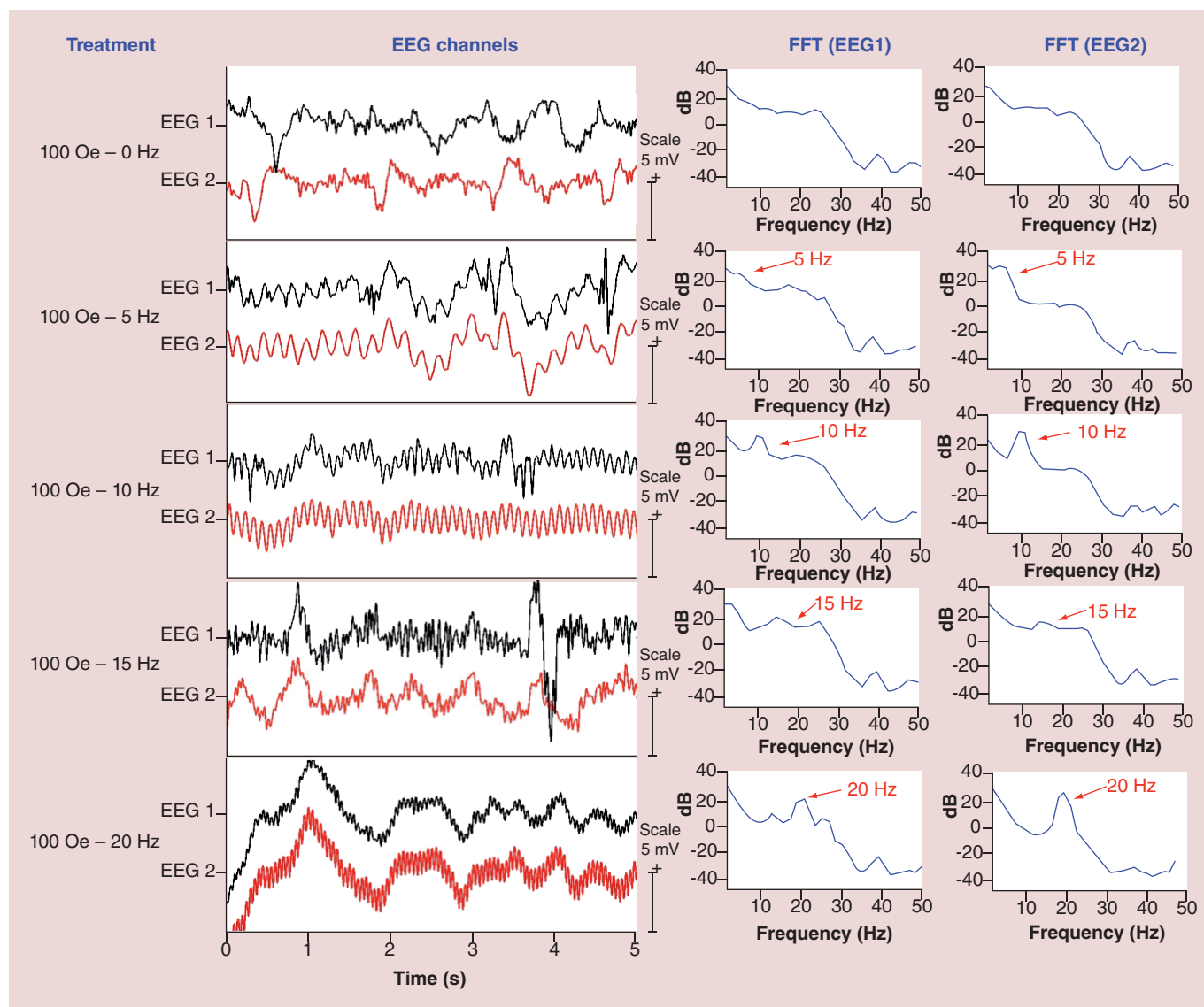


Figure 3. Key measurements – EEG waveforms with magnetolectric nanoparticles in the brain. EEG waveforms (left) and their frequency spectra (right) from the two EEG channels with MENs in the brain under exposure to an external 100-Oe a.c. magnetic field at frequencies of 0, 5, 10, 15 and 20 Hz. The vertical scale bar for the waveform signal is 5 mV.

be assumed that MENs undergo a similar metabolism as these conventional nanoparticles do. In addition, the current study can not provide the information on the distribution of the nanoparticles in different cells in different brain regions, for example, cerebral vascular cells, lymphocytes, astrocytes and others. In a first-order approximation, the distribution can be assumed to be similar to the distribution of long-circulating PEGylated cyanoacrylate nanoparticles [24]. Finally, it is worth noting that the novel nanotechnology allows using external magnetic fields to determine the location of the stimulation regions deep in the brain. One potential approach to accomplish the spatial selectivity might be the implementation of multiple coherent near-field antennas which operate in a hologram-like regime.

As noted above, MENs, unlike MNs, have an entirely new property due to the ME coupling. Because of its intrinsic nature, the coupling is relatively energy efficient. For example, considering the value for the ME coefficient, approximately $100 \text{ mV cm}^{-1} \text{ Oe}^{-1}$, according to a trivial isotropic expression for the ME effect, $\Delta P = \alpha H$, where P and H stand for the induced electric dipole field and the external magnetic field, respectively, an electric field on the order of 100 V/m could be generated a few nanometers away from a MEN merely by applying a weak magnetic field of 100 Oe . This would be a conservative estimate, because no contribution of the edge effects due to the deviation of the nanoparticle's shape from an elliptical configuration was taken into account. It can be noted that the magnitude of this

induced local electric field is comparable to that of the electric field due to the normal neural activity in the brain, for example, displayed as action potentials. Previously, using an example of patients with Parkinson's disease, we have theoretically shown that indeed the ME coupling in intravenously injected MENs could be used to stimulate the brain via remote application of a relatively low magnetic field (~ 100 Oe) in the near d.c. frequency range ($\sim <100$ Hz) to the same level achieved via the highly invasive conventional DBS [5]. In this case, each MEN in the brain serves as a highly localized high-efficacy converter of a weak external magnetic field into a high internal electric field; consequently, ideally the functions in the brain could be controlled at the subneuronal level provided the nanoparticle dosage and spatial distribution are selected so that at least a few nanoparticles are present per each neuron. Still, an important milestone of proving the concept experimentally and particularly through *in vivo* measurements was achieved only in the current study.

The two EEG channels, which were surgically attached to the head, could directly measure the local electric signals in two regions of the brain. As predicted, using an externally applied a.c. magnetic field with an amplitude of only 100 Oe and in a frequency range from 0 to above 20 Hz, we could significantly modulate the two EEG waveforms with the frequency of the external a.c. magnetic field (Figure 3). The amplitude of the modulated sinusoidal signal at four frequency values, 5, 10, 15 and 20 Hz, respectively, was comparable to the magnitude of the original nonmodulated signal at the same locations. The fact that the modulation amplitude saturated at an a.c. external magnetic field of 100 Oe (Figure 4), which was comparable to the coercivity of MENs, was in agreement with the assumption that the electric-field stimulation was triggered by the signal coming from MENs due an externally generated magnetic field. At the same time, the fact that the a.c.-induced modulation signal disappeared after the mouse was euthanized indicates that the modulation signal indeed originated from the active neural network and was not caused merely by an inductive coupling between MENs and the EEG probes.

To further ensure that this modulated signal was caused by the presence of MENs in the brain and did not originate from the electrical setup contacts/connections or other sources, we conducted equivalent control measurements without any injected nanoparticles (Supplementary Figure 3). Indeed, no detectable frequency modulation was observed in this case. Here, it should be reminded that to avoid any signal interference due to any residual nanoparticles in the brain, each new set of measurement conditions was tested on a new mouse. Finally, to compare MENs to the conventional

MNs that do not display the ME effect, another control study was conducted; a similar dose of MNs was administrated according to the above standard procedures (Supplementary Figure 4). These 30-nm MNs were made of a high-moment CoFe_2O_4 composition, with a coercivity of 100 Oe and a saturation magnetization of 100 emu/g. The applied a.c. field of 100 Oe was comparable to the coercivity field for MNs. As a result, because of the relatively high saturation magnetization value, MNs in their proximity were expected to regenerate a magnetic field on the order of 1000 Oe, in other words, at least an order of magnitude higher than the externally applied field. It is known that such high magnetic fields can indeed stimulate the brain. For example, the above discussed rTMS approach is based on such high fields. Nevertheless, compared with the modulation signal due to MENs, the signal due to MNs was below the detection level of approximately 50 μV . This observation is in agreement with the significantly stronger magnetic-to-electric-field coupling in the case of MENs due to the intrinsic nature of this coupling. Strikingly, in this comparison between MENs and MNs, the saturation magnetization of MENs was two orders of magnitude smaller than that of MNs; the latter indicates that the effect of the MEN-generated local electric field overshadows the effect of the MN-re-generated local magnetic field. Unlike stimulation with MNs or rTMS, stimulation with MENs did not require a high external magnetic field on the order of 10^4 Oe and instead originated from a significantly enhanced local high electric field only a few nanometers away from the nanoparticles which were exposed to a 100 Oe external magnetic field. Apparently, because there are hundreds of nanoparticles per neuron, the MENs' contribution is adequately strong to trigger the observed significant neural stimulation.

Though both MNs and MENs respond to an external magnetic field, they respond differently. When exposed to a magnetic field, MNs can locally regenerate an even stronger magnetic field. The field amplification factor, β , is proportional to the ratio of the saturation magnetization, M_s , and the magnetic anisotropy field, H_K , in other words, β approximately $4\pi M_s/H_K$. For example, for typical iron-oxide-based nanoparticles with $4\pi M_s$ on the order of 1000 emu/cc and H_K on the order of 100 Oe, the local amplification factor would be on the order of 10 and therefore the locally amplified magnetic field would be on the order of 1000 Oe. In turn, the higher local magnetic field implies the stronger coupling to intrinsic electric currents due to the local neural activity. As for MENs, under the same magnetic field exposure, not only they modify the local magnetic field but also generate a local electric field. Therefore, because the neural system is inherently

electric-field driven, these new ‘smart’ nanoparticles can provide substantially stronger coupling to the system. In fact, typical MENs have a substantially smaller value of the saturation magnetization (often, a couple of orders of magnitude smaller) compared with that of typical magnetic nanoparticles; thus, in case of MENs, the magnetically induced electric field action can substantially overshadow the purely magnetic field action. In summary, while in theory both MNs and MENs could solve the current problem of the weak coupling between external magnetic fields and CNS’s internal electric fields, MENs could provide a more intricate coupling to CNS compared with that by MNs.

Because the two nanoparticle systems under study, in other words, MNs and MENs, have a nonzero magnetic moment, ideally, they can be detected via existing magnetic imaging techniques such as the conventional MRI or the state-of-the-art magnetic nanoparticle imaging (MNI) [28–30]. If the concentration of nanoparticles is high enough to ensure that at least a few of them are present in each neuron, then, when exposed to a local magnetic field, the selected brain region would be stimulated without a need for the above conventional invasive contact-based DBS or relatively inefficient high-field TMS procedures. In other words, by introducing the magnetoelectric nanoparticles in the brain, we effectively create a new ‘nanoenvironment’ in which intrinsic electric signals in CNS are robustly coupled to an external magnetic field at the subneuronal level. Such an energy-efficient external connection to the brain could potentially open an unprecedented pathway to control selective brain regions; magnetic imaging techniques such as MNI or MRI could be used for both 3D imaging and selective local stimulation on demand by localizing fields via special magnetic coils. (Here, it could be mentioned that MNI might be more suitable

for being used with MENs because of the potential for superior sensitivity and real-time resolution capability.) The basic steps of the main concept are illustrated in schematics in Figure 5.

The current study was focused on the concept demonstration. To further underscore the significance of this study, it is worth noting that introduction of MENs in the brain could open a pathway for ‘writing’ and ‘reading back’ an electric field map of the brain at a subneuronal level. Such 3D electric-field mapping via MENs can be used for both remote stimulation of specific functions and ‘reading back’ the electric field information with a subneuronal precision, of course, provided there is an adequate magnetic imaging technique available. For example, one important future application of the unprecedented capability would be to use MENs in conjunction with existing magnetic imaging approaches, for example, MRI or MNI (suitable for real time monitoring), to enable ‘pinpoint’ diagnostic and therapy. While magnetic imaging using MENs as contrast agents would be modulated with local electric fields due to the neural activity and therefore would provide a real-time electric field map of the brain, a focused low-energy a.c. magnetic field could be used to stimulate/treat any specific region deep in the brain in a ‘pinpoint’ fashion. Theoretically, according to the Principle of Reciprocity, proving the validity of one of the two ways, ‘writing’ or ‘reading back’ information in the brain, respectively, can lay ground for proving the validity of the other [31]. The focus of this particular study was to prove that the brain could be ‘written’ (stimulated) through an external field. Specifically, we demonstrated that with MENs, because of their strong ME coupling, a portable-battery-driven and relatively small size coil could generate an external magnetic field that is strong enough to stimulate intrinsic electric signals in the CNS deep in the brain. Finally, it could be noted that the MEN’s parameters are not limited to the CoFe_2O_4 – BaTiO_3 composition and the 30-nm diameter, as used in the current study. It is likely that the concept could be further improved through using different materials, for example, biodegradable compositions, and even smaller size nanoparticles.

Conclusion

In summary, to the best of our knowledge, this *in vivo* study for the first time demonstrated the unprecedented potential of MENs to externally incite deep-brain neural stimulation. At least 10 μg of nanoparticles, which were iv.-injected in the blood stream through the tail vein of an ICR mouse, were forced to cross the BBB via application of a d.c. magnetic field gradient of 3000 Oe/cm. Through a surgically attached two-channel EEG headmount, an *in vivo* experiment demonstrated that

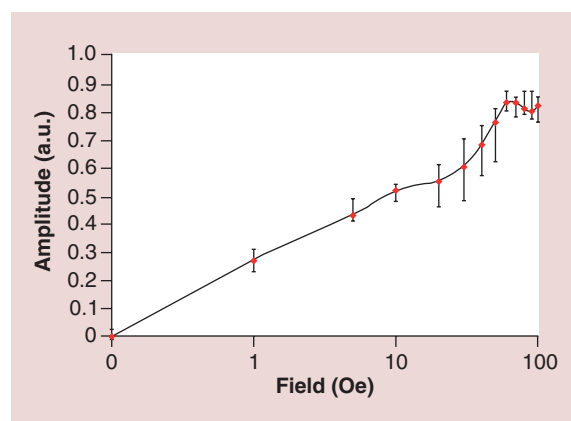


Figure 4. a.c. field dependence of the modulation effect. The modulation amplitude of the electric signal (in arbitrary units) versus the external a.c. magnetic field amplitude. The field axis is shown in a logarithmic scale.

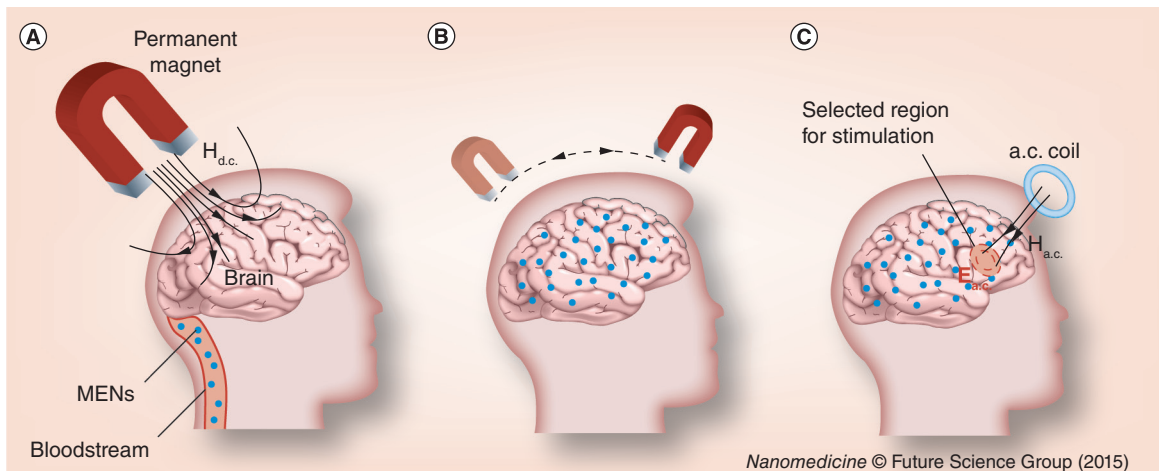


Figure 5. Concept illustration. Schematic illustration of the novel concept to use MENs for 'mapping' the brain for noninvasive electric field stimulation of selected regions deep in the brain. **(A)** MENs are forced into the brain across blood–brain barrier via application of a d.c. magnetic field gradient. **(B)** When in the brain, MENs are being distributed over the entire brain or in selected regions via application of spatially varying d.c. magnetic field gradients. The presence of MENs effectively creates a 'new brain microenvironment', in which the intrinsic electric signals due to the neural activity are strongly coupled at the subneuronal level to the external magnetic fields generated by remote sources. **(C)** Such coupling can be used for noninvasive high-efficacy stimulation of selected regions deep in the brain via application of focused and relatively low (~ 100 Oe) near-d.c. ($\sim <1000$ Hz) magnetic field.

MEN: Magnetoelectric nanoparticle.

the administrated MENs could modulate the electric waveforms deep in the brain via application of a 100-Oe a.c. magnetic field in a frequency range from 0 to 20 Hz. Control measurements with mice, in which instead of MENs conventional high-moment magnetic nanoparticles were administrated and no nanoparticles were administrated, showed no significant modulation.

Future perspective

The described study is a stepping stone toward the development of a personalized nanotechnology for simultaneously achieving the following three important functions: stimulation; release of drug(s) and other macromolecule(s), for example, peptides, RNAs and others, in selective brain regions via remote control and mapping the electric field due to neural activity. Achieving each of these functions would be an important milestone on its own. Achieving all these three functions simultaneously would open a pathway to the next-generation pinpoint treatment of neurological diseases such as Parkinson's, Alzheimer's, Autism, and others. This study has demonstrated the feasibility of using MENs as externally controlled 'smart' nanoparticles that could potentially be used for navigation and selective control of specific functions deep in the brain. Even more far-reaching applications might be envisioned when biodegradable MENs will be developed in the future, which is definitely not out of reach due to the recent development in the emerging field of carbon based nanotechnology. The potential applica-

tions span from the prevention and treatment of neurodegenerative disorders to opening a pathway to significantly improving our fundamental understanding of the brain and reverse-engineering the brain [32].

Acknowledgements

The authors thank Horatiu Venerian for his continuous support during animal studies and Erasmo Perera for preparing brain sections.

Financial & competing interests disclosure

The authors acknowledge partial financial support from National Science Foundation (NSF) awards #ECCS-1408063 and IIP-1237818, NIH DA #R01DA034547-01 and Department of Defense (DoD) Defense Microelectronics Activity (DMEA) under contract #H94003-09-2-0904. The authors have no other relevant affiliations or financial involvement with any organization or entity with a financial interest in or financial conflict with the subject matter or materials discussed in the manuscript apart from those disclosed.

No writing assistance was utilized in the production of this manuscript.

Ethical conduct of research

The authors state that they have obtained appropriate institutional review board approval or have followed the principles outlined in the Declaration of Helsinki for all human or animal experimental investigations. In addition, for investigations involving human subjects, informed consent has been obtained from the participants involved.

Executive summary

- The capability to externally control local electric fields due to the neural activity deep in the brain is hard to overestimate.
- The potential applications range from deep brain stimulation for treating neurodegenerative diseases to nanotechnology tools to understand the brain.
- In *in vivo* study on imprinting control region mice is conducted to show that magnetoelectric nanoparticles (MENs) may be able to address this subject. Due to the magnetoelectric effect, these 'smart' nanoparticles can directly couple intrinsic electric-field-driven processes with external magnetic fields for providing another dimension to control the neural activity.

Methods

- Toxicity-free MENs, made of CoFe₂O₄-BaTiO₃ core-shell 30-nm nanostructures coated with a 2-nm glycerol mono-oleate, were pulled into the brain via magnetic field gradient of 3000 Oe/cm.
- Scanning electron microscopy and magnetic force microscopy were used to detect nanoparticles in brain sections of imprinting control region mice.
- A surgically attached electroencephalography headmount was used to confirm MEN-induced stimulation via application of an external magnetic field of 100 Oe in a frequency range from 0 to 30 Hz.

Results & conclusions

- The presence of MENs in the brain was confirmed via the above two imaging methods.
- An external a.c. magnetic field modulated electroencephalography signal by a 1-mV a.c. signal.
- The modulation signal depended on the external field frequency and amplitude, with a saturation field of 100 Oe.

References

Papers of special note have been highlighted as: • of interest

- 1 Marblestone AH *et al.* Physical principles for scalable neural recording. *Front. Comput. Neurosci.* 7, 137 (2013).
- Gives a unique technology angle on the current state of neuroengineering.
- 2 Hopfield JJ. Neurons with graded response have collective computational properties like those of two-state neurons. *Proc. Natl Acad. Sci. USA* 81, 3088–3092 (1984).
- 3 De Kramer J. The electrical circuitry of an olfactory sensillum in *Antheraea polyphemus*. *J. Neurosci.* 5, 2484–2493 (1985).
- Presents the concept of the brain's electric circuitry.
- 4 Srikanth M, Kessler JA. Nanotechnology – novel therapeutics for CNS disorders. *Nat. Rev. Neurol.* 8, 307–318 (2012).
- Gives an overview of using nanotechnology for treating central nervous system disorders.
- 5 Yue K *et al.* Magneto-electric nano-particles for non-invasive brain stimulation. *PLoS ONE* 7, e44040 (2012).
- Gives a theoretical insight into using magnetoelectric nanoparticles for noninvasive brain stimulation.
- 6 Brambilla D, Le Droumaguet B, Nicolas J *et al.* Nanotechnologies for Alzheimer's disease: diagnosis, therapy, and safety issues. *Nanomedicine* 7, 521–540 (2011).
- 7 Kringelbach ML, Jenkinson N, Owen SL, Aziz TZ. Translational principles of deep brain stimulation. *Nat. Rev. Neurol.* 8, 623–635 (2007).
- 8 Stefani A *et al.* Bilateral deep brain stimulation of the pedunculopontine and subthalamic nuclei in severe Parkinson's disease. *Brain* 130, 1596–1607 (2007).
- 9 Schlaepfer TE *et al.* Deep brain stimulation to reward circuitry alleviates anhedonia in refractory major depression. *Neuropsychopharmacology* 33, 368–377 (2008).
- 10 Barker AT, Jalinous R, Freeston IL. Non-invasive magnetic stimulation of human motor cortex. *Lancet* 325, 1106–1107 (1985).
- 11 Pascual-Leone A. Transcranial magnetic stimulation: studying the brain-behaviour relationship by induction of 'virtual lesions'. *Philos. Trans. R. Soc. Lond. B Biol. Sci.* 354, 1229–1238 (1999).
- 12 Nitsche MA, Paulus W. Sustained excitability elevations induced by transcranial DC motor cortex stimulation in humans. *Neurology* 57, 1899–1901 (2001).
- 13 Boggio PS, Ferrucci R, Rigonatti SP *et al.* Effects of transcranial direct current stimulation on working memory in patients with Parkinson's disease. *J. Neurol. Sci.* 249, 31–38 (2006).
- 14 Fregni F, Pascual-Leone A. Technology insight: noninvasive brain stimulation in neurology – perspectives on the therapeutic potential of rTMS and tDCS. *Nat. Clin. Pract. Neuro.* 3, 383–393 (2007).
- 15 Yoo SS, Bystritsky A, Lee JH *et al.* Focused ultrasound modulates region-specific brain activity. *Neuroimage* 56, 1267–1275 (2011).
- 16 Huang YZ, Sommer M, Thickbroom G *et al.* Consensus: new methodologies for brain stimulation. *Brain Stimul.* 2, 2–13 (2009).
- 17 Coenen AM. Neuronal activities underlying the electroencephalogram and evoked potentials of sleeping and waking: implications for information processing. *Neurosci. Biobehav. Rev.* 19, 447–463 (1995).
- 18 Zhao Z, Zhou Z, Bao J. Octapod iron oxide nanoparticles as high-performance T2 contrast agents for magnetic resonance imaging. *Nat. Commun.* 4, 2266 (2013).
- 19 Corral-Flores V, Bueno-Baques D, Ziolo R. Synthesis and characterization of novel CoFe₂O₄-BaTiO₃ multiferroic core-shell-type nanostructures. *Acta Mater.* 58, 764–769 (2010).

- 20 Kitagawa Y, Hiraoka Y, Honda T, Ishikura T, Nakamura H, Kimura T. Low-field magnetoelectric effect at room temperature. *Nat. Mater.* 9, 797–802 (2010).
 - 21 Luo W *et al.* Room-temperature simultaneously enhanced magnetization and electric polarization in BiFeO₃ ceramic synthesized by magnetic annealing. *Appl. Phys. Lett.* 94, 202507 (2009).
 - 22 Nair M, Guduru R, Liang P, Hong J, Sagar V, Khizroev S. Externally controlled on-demand release of anti-HIV drug using magneto-electric nanoparticles as carriers. *Nat. Commun.* 4, 1707 (2013).
 - 23 Guduru R, Khizroev S. Magnetic field-controlled release of paclitaxel drug from functionalized magnetoelectric nanoparticles. *Part. Part. Syst. Char.* 31(5), 605–611 (2013).
 - 24 Calvo P, Gouritin B, Chacun H *et al.* Long-circulating PEGylated polycyanoacrylate nanoparticles as new drug carrier for brain delivery. *Pharm. Res.* 18(8), 1157–1166 (2001).
 - 25 Guduru R, Liang P, Runowicz C, Nair M, Alturi V, Khizroev S. Magnetoelectric nanoparticles to enable field-controlled high-specificity drug delivery to eradicate ovarian cancer cells. *Sci. Rep.* 3, 2953 (2013).
 - 26 Eskandar E, Rabinov J, Barker FG. Tracking neural stem cells in patients with brain trauma. *N. Engl. J. Med.* 355(22), 2376–2378 (2006).
 - 27 Kim DK, Zhang Y, Kehr J, Klason T, Bjelke B, Muhammed M. Characterization and MRI study of surfactant-coated superparamagnetic nanoparticles administrated into the rat brain. *J. Mag. Mag. Mat.* 225, 256–261 (2001).
 - 28 Goodwill PW, Scott GC, Stang PP, Conolly SM. Narrowband magnetic particle imaging. *IEEE Trans. Med. Imaging* 28, 1231–1237 (2009).
 - 29 Weizenecker J, Gleich B, Rahmer J, Dahnke H, Borgert J. Three-dimensional real-time *in vivo* magnetic particle imaging. *Phys. Med. Biol.* 54, L1 (2009).
 - 30 Yassa MA, Muftuler LT, Stark CE. Ultrahigh-resolution microstructural diffusion tensor imaging reveals perforant path degradation in aged humans *in vivo*. *Proc. Natl Acad. Sci. USA* 107, 12687–12691 (2010).
 - 31 Khizroev SK, Bain JA, Kryder MH. Considerations in the design of probe heads for 100 Gbit/in² recording density. *IEEE. Trans. Magn.* 33, 2893–2895 (1997).
 - 32 Koch C, Tononi G. Can machines be conscious? *IEEE Spectrum* 45(6), 55 (2008).
- **Presents a concept of reverse-brain engineering.**